Topology and Control of the Fault-Tolerant DC-DC Converter for Fuel Cell Application

Shengrong Zhuo, Arnaud Gaillard, Damien Paire, and Fei Gao
FEMTO-ST Institute, Univ. Bourgogne Franche-Comté, UTBM, CNRS, Belfort 90010, France
E-mail: {shengrong.zhuo, arnaud.gaillard, damien.paire, fei.gao}@utbm.fr

ABSTRACT -In this paper, a robust controller is proposed for a fault-tolerant dc-dc converter for fuel cell application, to deal with the adverse effects caused by the switch fault. First, the dc-dc converter topologies for fuel cell applications with switch fault tolerance are discussed. Then, the converter topology is properly selected. Finally, a hybrid dual-loop controller based on active disturbance rejection algorithm and super-twisting algorithm is elaborated. Both the simulation and experimental results are presented. The proposed controller can achieve almost consistent performance in converter healthy mode and post-fault mode without needing fault diagnosis information.

Keywords—DC-DC converter, fault tolerance, robust control, active disturbance rejection control, fuel cell application.

1. INTRODUCTION

The fuel cell is a device that can convert the chemical energy stored in the reactant gas into electricity, with the only byproducts of heat and water. It is considered as a kind of energy of zero-emission and has been getting more and more utilization in industry applications. The application range is as diverse as portable devices, stationary power generation systems, data centers, vehicles, railway, and other transportation tools. Be similar to many other new energy sources, the output voltage of the fuel cell is relatively low and varied [1]. Therefore, to meet the load requirement, it is of great necessity to interface with a step-up dc-dc power converter to regulate a stiff dc bus [2].

According to the survey reported in [3], the power switch is one of the most fragile components within power converters, it takes up about 30% of the malfunctions. Therefore, to ensure the longtime and stable converter operation, the switch failure issue is an important concern. To this end, the solutions are twofold. The first thing is to construct a converter with switch redundancy, realized by either the inherent topology or adding the back-up switch. Most of the papers available in the literature focus mainly on the converters with high step-up ratio [2], [4]. Therefore, in the first part of this paper, the converters for fuel cell applications, in particular that with switch redundancy, are briefly discussed.

The second thing is to develop a fault-tolerant control to ensure the post-fault converter operation. The fault-tolerant control is generally distinguished as passive fault-tolerant control and active fault-tolerant control [5]. The active fault-tolerant control is designed on the basis of fault diagnosis [6]. Two (or more) controllers are designed for the converter in healthy mode and switch fault mode, respectively. After diagnosing the switch fault via the fault diagnosis module, the controller gain is switched. In [7], this control is designed for a three-phase interleaved boost converter. The results show that the converter has good performance before and after the switch fault. The effectiveness of this kind of control depends largely on the fault diagnosis module. The false alarm of fault diagnosis may lead to degraded performance or even unstable system. The idea of passive fault-tolerant control is to develop a controller that can be used in both healthy case and post-fault case. It uses the controller robustness to deal with the adverse effect of switch fault, resulting in much higher requirements for the controller.

In this paper, a robust hybrid dual-loop controller based on active disturbance rejection algorithm and super-twisting sliding mode algorithm is designed for a fault-tolerant dc-dc converter for fuel cell application. Due to the strong robustness of the proposed controller, it can well deal with the adverse effects caused by the switch fault. It can be used for the converter under both healthy mode and switch fault mode.

The rest of the paper is organized as follows. In Section 2, the converter topologies with switch fault tolerance are discussed. In Section 3, the converter analysis and modeling of the selected converter are presented. In Section 4, a robust passive fault-tolerant control is elaborated, and the obtained results are shown. Finally, Section 5 is a conclusion.

2. TOPOLOGY OF THE CONVERTER FOR FUEL CELL APPLICATION

The dc-dc converters for fuel cell application generally need to meet the requirements of [8], [9]: 1) low input current ripple; 2) low component stress; 3) high converter efficiency; 4) high reliability; 5) high voltage gain.

Associating the basic dc-dc converters based on the input-parallel output-parallel (IPOP) structure is a typical choice, see Fig. 1(a). The basic dc-dc converter unit is regarded as a cell within the interleaved converter. Fig. 1(b) shows a two-phase interleaved boost converter, in which the boost converter is the basic cell. As observed in Fig. 2, the interleaved converter can reduce considerably the input current ripple, by utilizing phase shifting, without the use of extra hardware. Moreover, the current distribution between phases alleviates largely the component current stress, and improves the energy conversion efficiency and heat distribution. The reliability study in [10] shows that the interleaved converter in Fig. 1(b) features higher reliability. Due to the inherent redundancy, it can continue operating even after a switch fault.

The interleaved boost converter of IPOP structure has the same voltage ratio as that of the basic converter cell, and the component voltage stress is not reduced as well, which equals to the output voltage. Therefore, combining the basic dc-dc converters via the input-parallel output-series (IPOS) structure is proposed, as shown in Fig. 3(a). It needs to note that only the isolated converter can work directly as a cell in this structure. For the preferred nonisolated converter, if the input-side and output-side share the same ground, one can first obtain a similar converter using mirrored symmetry, then combine the original converter and the mirrored one via IPOS structure. An example based on the boost converter is plotted in Fig. 3(b) for illustration [11], [12].

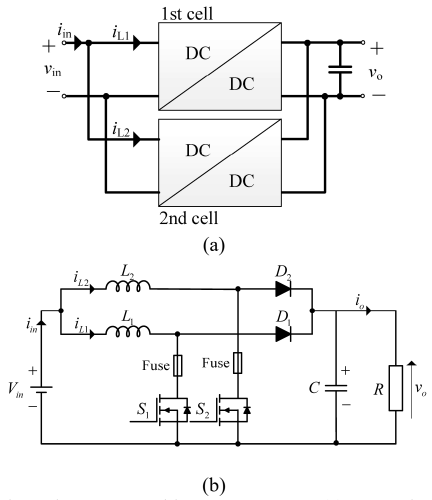

Fig. 1. Interleaved converter with IPOP structure. (a) General structure. (b) Topology of the interleaved boost converter.

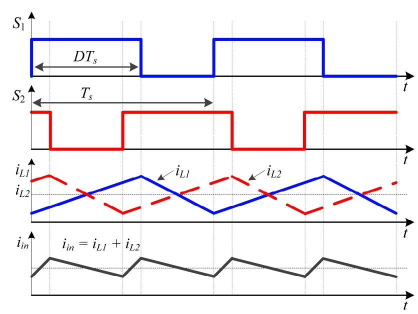

Fig. 2. Phase interleaving to reduce the input current ripple.

The IPOS structure preserves the main advantages of the IPOP structure, for example, the low input ripple. Meanwhile, it can increase the voltage step-up ratio and reduce the voltage rating of the converter components. To further improve voltage gain and reduce the component voltage stress, various voltage step-up techniques [13], such as cascade method, voltage lift, switched capacitor, coupled inductor, and voltage multiplier are reported in the literature, which can integrate into each cell or between the cells. A general concept topology, based on input-parallel structure and various step-up techniques, is summarized in Fig. 4. It needs to highlight that these step-up techniques help to improve the converter voltage gain, at the cost that the circuit complexity is also increased. Therefore, a careful balance should be taken between the voltage gain and the converter circuit

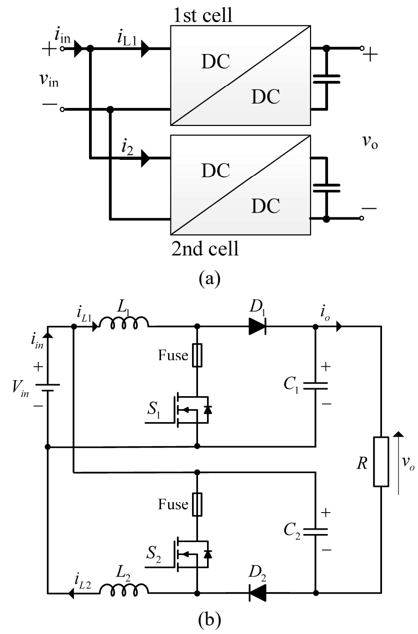

Fig. 3. Interleaved converter with IPOS structure. (a) General structure. (b) Topology of the interleaved boost converter.

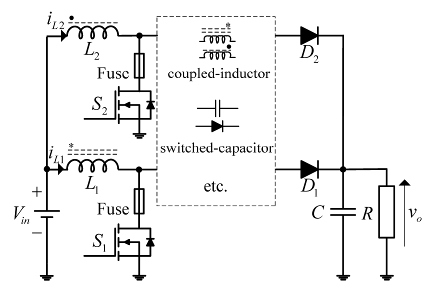

Fig. 4. Concept of the interleaved converter with integrated step-up circuit.

complexity in selecting the appropriate topology. In this paper, the converter topology shown in Fig. 3(b) is chosen and studied.

3. Converter Analysis and Converter Modeling

3.1. Converter in healthy mode

The output voltage of the converter in Fig. 3(b) satisfies:

$$v_o = v_{C1} + v_{C2} - v_{in} \tag{1}$$

where v_{in} is the input voltage, v_{C1} and v_{C2} are the terminal voltage of the capacitor C_1 and C_2, respectively.

The symmetrical cells are considered, thus, there are:

$$L_1 = L_2 = L, C_1 = C_2 = C, d_1 = d_2 = D \tag{2}$$

where D is the duty cycle of the switch.

The capacitor voltage and inductor current are:

$$V_{C1} = V_{C2} = \frac{V_o}{1+D}, I_{L1} = I_{L2} = \frac{I_{in}}{1+D} \tag{3}$$

The voltage gain of the ideal converter is:

$$M(D) = \frac{V_o}{V_{in}} = \frac{1+D}{1-D} \tag{4}$$

3.2. Converter in switch fault mode

The converter can continue operating after switch fault. Consider the case that the switch fault occurs in switch S_2, the capacitor voltage and inductor current become:

$$V_{C1} = V_o, V_{C2} = V_{in}, I_{L1} = I_{in}, I_{L2} = I_o \qquad (5)$$

The above equations mean that the converter needs to sustain higher voltage and current stress under switch fault mode. Therefore, the component oversizing needs to be considered in operating the converter in switch fault mode.

3.3. Converter modeling

The average model of the converter can be expressed as:

$$\begin{cases} L\frac{di_{Lk}}{dt} = v_{in} - (1-d_k)v_{Ck} \\ C\frac{dv_{Ck}}{dt} = (1-d_k)i_{Lk} - i_o \end{cases} \qquad (6)$$

where $k = 1, 2$.

4. CONTROL OF A FAULT-TOLERANT DC-DC CONVERTER

The converter introduced in Fig. 3(b) naturally has switch redundancy, it is thus possible to achieve switch fault tolerance and continuous operation by designing a proper controller. The methods to ensure good converter performance in both healthy mode and switch fault mode can mainly be divided into two categories: active fault tolerant control and passive fault-tolerant control. The active fault tolerant control consists of fault detection and diagnosis, and fault reconfiguration. The effectiveness of this kind of control depends largely on the fault diagnosis module. The false diagnosis leads to converter degraded performance or instability. Therefore, in this section, a robust hybrid dual-loop controller based on active disturbance rejection control and super-twisting sliding mode algorithm, which can be regarded as a kind of passive fault-tolerant control, is designed. It can achieve good converter performance in both healthy mode and switch fault mode.

4.1. Controller scheme

The converter for fuel cell application needs to satisfy the control goals of the constant voltage regulation, current sharing between phases, and phase interleaving to reduce the input current ripple. It also needs to ensure continuous operation after switch fault. Fig. 5 shows the proposed dual-loop control scheme. The outer-loop voltage controller regulates the output voltage to the desired reference value. The inner-loops regulate the inductor current, respectively. The two current controllers share the same current reference, the equal current sharing is thus guaranteed. The carries in PWM 1 and PWM 2 blocks are phase-shifted evenly by 180°. In addition, after the switch fault, the rest healthy phase would compensate for the lost phase to realize the continuous operation.

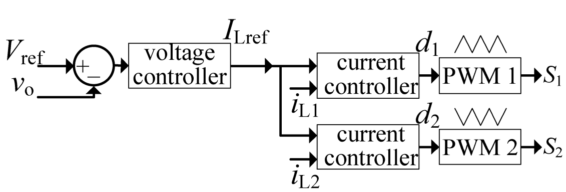

Fig. 5. Control scheme of the converter. PWM: Pulse width modulation.

4.2. Controller design

In this paper, to obtain better dynamic performance, the inner-loop current controller is designed based on super-twisting sliding mode control law [14], and the output-loop voltage controller is devised based on active disturbance rejection control algorithm [15]. The proposed hybrid dual-loop controller is expressed as follows.

Inner-loop:

$$d_k = \lambda_k(I_{Lref} - i_{Lk}) + \alpha_k \int sgn(I_{Lref} - i_{Lk})dt \qquad (7)$$

where d_k is the duty cycle for the switch S_k, k = 1,2. λ_k, α_k are controller parameters, i_{Lk} is the inductor current flowing through the inductor L_k. sgn(x) is a stand *sign* function of the variable x.

Outer-loop:

$$\begin{cases} I_{Lref} = \frac{k_p(V_{ref}-v_o)-z_2}{b_0} \\ \dot{z}_1 = z_2 + b_0 I_{Lref} + g_1(y - z_1) \\ \dot{z}_2 = g_2(y - z_1) \end{cases} \qquad (8)$$

where b_0, g_1, g_2 are controller parameters. V_{ref} is the output voltage reference, v_o is the output voltage. To deal with the cases of healthy converter and switch fault converter, the controller parameter b_0 is adapted as [16]:

$$b_0 = \frac{1}{C}\left((1-d_1) + (1-d_2)\right) \qquad (9)$$

where C is the capacitance.

4.3. Simulation results

Based on the Matlab/Simulink, the converter is constructed using the circuit parameters $L_k = 400\mu\text{H}$, $C_k = 1000\mu\text{F}$, as shown in Table I. The proposed controller is implemented with the parameters $\lambda_k = 0.05$, $\alpha_k = 60$, $g_1 = 800$, $g_2 = 160000$. The output voltage reference is 48V. The obtained results are presented in Fig. 6 and Fig. 7.

TABLE I
CIRCUIT PARAMETER OF CONVERTER

Item	Value
Rated input voltage V_{in}	16 V
Output voltage V_o	48 V
Nominal load R	100 Ω
Inductor L	400 µH
Inducotr resistor r_L	0.43 Ω
Capacitor C	1000 µF
Capacitor resistor r_C	0.04 Ω
Switching frequency f_s	25 kHz

As shown in Fig. 6, the input voltage disturbance $v_{in} = 16 + 4\sin(20\pi t)\text{V}$ is applied, and the value of b_0 is adapted accordingly. It is observed that the proposed controller has good voltage regulation in both converter healthy mode and switch fault mode, verifying the superior performance of the proposed controller.

The switch fault transient result is displayed in Fig. 7. It is seen that the value of b_0 can adapt accordingly to deal with the effect of switch fault. Moreover, the output voltage can maintain at the reference value 48V after a short transient, demonstrating the high reliability of the presented converter and the effectiveness of the proposed controller. At the start, the two inductor currents are equal. After the switch fault at t = 0.3s, the inductor current of fault phase i_{L2} suddenly reduces to zero. It later increases to be equal to the load current due to the operation principle of the topology [4].

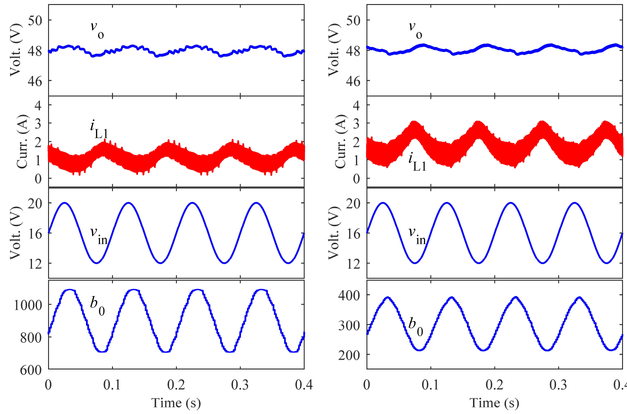

(a) (b)

Fig. 6 Simulation results of the converter with the proposed controller. (a) converter healthy mode. (b) switch fault mode (fault occurs in switch S_2).

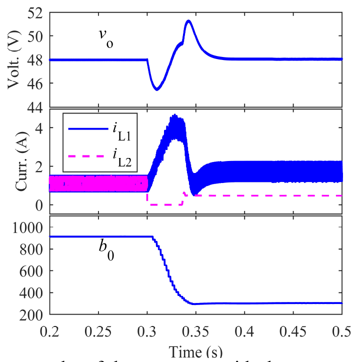

Fig. 7 Simulation results of the converter with the proposed controller during switch fault transient, fault occurs in switch S_2 at $t = 0.3$s.

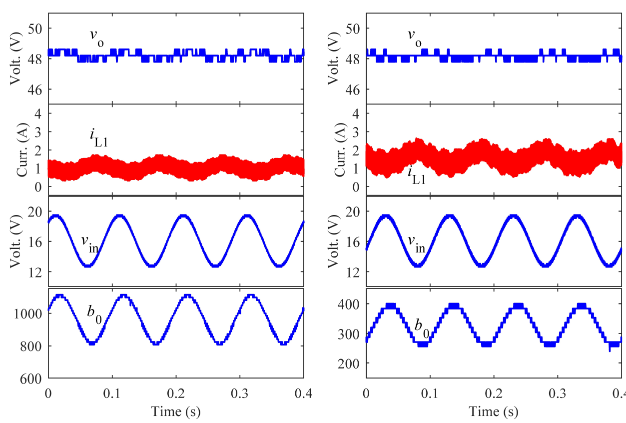

(a) (b)

Fig. 8 Experimental results of the converter with the proposed controller. (a) converter healthy mode. (b) switch fault mode (fault occurs in switch S_2).

4.4. Experimental results

The converter prototype is established to experimentally validate the proposed controller. The converter circuit parameter configuration is the same as that in the simulations. The switching frequency is 25 kHz. The dual-loop controller is implemented into the dSPACE. The obtained experimental results are shown in Fig. 8 and Fig. 9.

Fig. 8 shows the experimental results when the input voltage varying in the form of $v_{in} = 16 + 4\sin(20\pi t)$V. It is seen that it is consistent with the simulation results. The parameter b_0 can well adapt with the input voltage change, and the output voltage can be regulated around the reference value 48 V, no matter in healthy mode or switch fault mode.

Fig. 9 presents the experimental results of the converter during switch fault transient. It is seen that similar to the simulation results of Fig. 7, the parameter b_0 can adapt accordingly, and the output voltage can recover to the reference value after a transient.

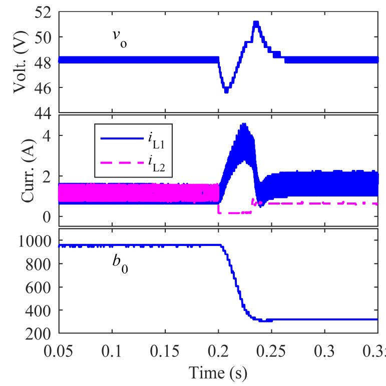

Fig. 9 Experimental results of the converter with the proposed controller during switch fault transient, fault occurs in switch S_2 at $t = 0.2$s.

5. Conclusions

A robust hybrid dual-loop controller based on the active disturbance rejection algorithm and super-twisting sliding mode algorithm is designed for a fault-tolerant dc-dc converter for fuel cell application. Due to the strong robustness of the proposed controller, it can well deal with the adverse effects caused by the switch fault. The results show that it can achieve almost consistent performance under converter healthy mode and switch fault mode, showing superior performance. It can operate continuously from healthy mode to switch fault mode. It needs to highlight that the switch fault would cause severe component stress, thus, the converter should be properly oversized in the converter design stage with switch fault consideration.

6. Acknowledgment

This work was supported by the region of Bourgogne Franche-Comté, France, under research agreement number 2017Y-06232/06241.

7. References

[1] F. Gao, B. Blunier, M. G. Simões and A. Miraoui, "PEM fuel cell stack modeling for real-time emulation in hardware-in-the-loop applications," *IEEE Transactions on Energy Conversion*, vol. 26, no. 1, pp. 184-194, March 2011.

[2] A. Kolli, A. Gaillard, A. De Bernardinis, O. Bethoux, D. Hissel, and Z. Khatir, "A review on DC/DC converter architectures for power fuel cell applications", *Energy Conversion and Management*, vol. 105, pp. 716-730, 2015.

[3] S. Yang, A. Bryant, P. Mawby, D. Xiang, L. Ran, and P. Tavner, "An industry-based survey of reliability in power electronic converters," *IEEE Transactions on Industry Application.*, vol. 47, no. 3, pp. 1441-1451, May-June 2011.

[4] F. L. Tofoli, D. d. C. Pereira, W. Josias de Paula and D. d. S. Oliveira Júnior, "Survey on non-isolated high-voltage step-up dc–dc topologies based on the boost converter," *IET Power Electronics*, vol. 8, no. 10, pp. 2044-2057, 10 2015.

[5] S. Zhuo, L. Xu, A. Gaillard, Y. Huangfu, D. Paire and F. Gao, "Robust open-circuit fault diagnosis of multi-phase floating interleaved dc–dc boost converter based on sliding mode observer," *IEEE Transactions on Transportation Electrification*, vol. 5, no. 3, pp. 638-649, Sept. 2019.

[6] J. Jiang, and X. Yu, "Fault-tolerant control systems: A comparative study between active and passive approaches," *Annuual Reviews in Control*, vol. 36, no. 1, pp. 60-72, 2012.

[7] E. Pazouki, J. A. De Abreu-Garcia and Y. Sozer, "A novel fault-tolerant control method for interleaved dc–dc converters under switch fault condition," *IEEE Transactions on Industry Applications*, vol. 56, no. 1, pp. 519-526, Jan.-Feb. 2020.

[8] M. Kabalo, B. Blunier, D. Bouquain and A. Miraoui, "State-of-the-art of DC-DC converters for fuel cell vehicles, " in *Proceedings of 2010 IEEE Vehicle Power and Propulsion Conference*, 2010, pp. 1-6.

[9] Q. Li, Y. Huangfu, L. Xu, J. Wei, R. Ma, D. Zhao, F. Gao, "An improved floating interleaved boost converter with the zero-ripple input current for fuel cell applications," *IEEE Transactions on Energy Conversion*, vol. 34, no. 4, pp. 2168-2179, Dec. 2019.

[10] A. Khosroshahi, M. Abapour and M. Sabahi, "Reliability evaluation of conventional and interleaved dc–dc boost converters," *IEEE Transactions on Power Electronics*, vol. 30, no. 10, pp. 5821-5828, Oct. 2015.

[11] Y. Huangfu, S. Zhuo, F. Chen, and S. Pang, "Evaluation and fault tolerant control of a floating interleaved boost converter for fuel cell systems," in *Proceedings of IEEE Industry Application Society Annuual Meeting*, 2016, pp. 1-7.

[12] S. Choi, V. Agelidis, J. Yang, D. Coutellier, and P. Marabeas, "Analysis, design and experimental results of a floating-output interleaved-input boost-derived dc-dc high-gain transformer-less converter," *IET Power Electronics*, vol. 4, no. 1, pp. 168-180, Jan. 2011.

[13] M. Forouzesh, Y. P. Siwakoti, S. A. Gorji, F. Blaabjerg, and B. Lehman, "Step-up dc–dc converters: A comprehensive review of voltageboosting techniques, topologies, and applications," *IEEE Transactions on Power Electronics*, vol. 32, no. 12, pp. 9143-9178, Dec. 2017.

[14] J. Han, "From PID to active disturbance rejection control," *IEEE Transactions on Industrial Electronics*, vol. 56, no. 3, pp. 900-906, March 2009.

[15] A. Levant, "Principles of 2-sliding mode design", *Automatica*, vol. 43, no. 3, pp. 576-586, 2007.

[16] S. Zhuo, A. Gaillard, L. Guo, L. Xu, D. Paire and F. Gao, "Active disturbance rejection voltage control of a floating interleaved dc–dc boost converter with switch fault consideration," *IEEE Transactions on Power Electronics*, vol. 34, no. 12, pp. 12396-12406, Dec. 2019.